

Tin-Capped Trinuclear Nickel Clusters: Redox Isomerism between μ_3 -Stannyl and μ_3 -Stannylene Clusters of the Class $[\text{Ni}_3(\text{dppm})_3(\mu_3\text{-I})(\mu_3\text{-SnCl}_x)]^{n+}$ ($x = 2, n = 1; x = 3, n = 0$)

Brian K. Breedlove,[†] Philip E. Fanwick,^{‡,§} and Clifford P. Kubiak^{*†}

Department of Chemistry and Biochemistry, University of California at San Diego, 9500 Gilman Drive, La Jolla, California 92093-0358, and Department of Chemistry, Purdue University, West Lafayette, Indiana 47907-1393

Received February 7, 2002

The reaction of $\text{Ni}_3(\text{dppm})_3(\mu_3\text{-I})_2$ with sodium trichlorostannate affords the first tin-capped nickel cluster $\text{Ni}_3(\text{dppm})_3(\mu_3\text{-I})(\mu_3\text{-SnCl}_3)$ (**1**). A site of coordinative unsaturation at tin can be introduced by the reaction of **1** with $\text{Ti}(\text{PF}_6)_4$ yielding the stannylene-capped cluster $[\text{Ni}_3(\text{dppm})_3(\mu_3\text{-I})(\mu_3\text{-SnCl}_2)]^+$ (**2**). Clusters **1** and **2** were characterized by ^{31}P NMR, X-ray diffraction, and cyclic voltammetry (CV). Clusters **1** and **2** exhibit single electron redox chemistries, $[\text{Ni}_3(\text{dppm})_3(\mu_3\text{-I})(\mu_3\text{-SnCl}_3)]^{0/+}$, $[\text{Ni}_3(\text{dppm})_3(\mu_3\text{-I})(\mu_3\text{-SnCl}_2)]^{+/0}$, that together comprise a redox equilibrium. Thus, electrochemical reduction of **1** produces first the $49e^-$ cluster radical anion $[\text{Ni}_3(\text{dppm})_3(\mu_3\text{-I})(\mu_3\text{-SnCl}_3)]^-$ which then yields the reduced form of **2**, $[\text{Ni}_3(\text{dppm})_3(\mu_3\text{-I})(\mu_3\text{-SnCl}_2)]$, upon chloride dissociation.

Cationic trinuclear nickel clusters of the type $[\text{Ni}_3(\mu_3\text{-CNR})(\mu_3\text{-I})(\mu\text{-dppm})_3]^+$ (R = alkyl, aryl; $\text{dppm} = \text{Ph}_2\text{PCH}_2\text{-PPh}_2$) catalyze the reduction of carbon dioxide in aprotic solvents at potentials near -1.2 V versus SCE.^{1,2} Kinetic evidence has been obtained that suggests CO_2 binds to a Ni_2 -($\mu_3\text{-L}$) face of the clusters.¹ Further advances in catalytic reduction of CO_2 may be realized with complexes that contain both nucleophilic and electrophilic reactive sites.^{3–6} Here, we describe the preparation, structure, and redox chemistry of the first *triangulo*-nickel clusters capped by tin.

* To whom correspondence should be addressed. E-mail: ckubiak@ucsd.edu.

[†] University of California at San Diego.

[‡] Purdue University.

[§] Address correspondence pertaining to crystallographic studies to this author. E-mail: fanwick@chem.purdue.edu.

- (1) Wittrig, R. E.; Ferrence, G. M.; Washington, J.; Kubiak, C. P. *Inorg. Chim. Acta* **1998**, *270*, 111–117.
- (2) Ratliff, K. S.; Lentz, R. E.; Kubiak, C. P. *Organometallics* **1992**, *11*, 1986–1988.
- (3) Gibson, D. H.; Ye, M.; Richardson, J. F. *J. Am. Chem. Soc.* **1992**, *114*, 9716.
- (4) Floriani, C.; Fachinetti, G. *J. Chem. Soc., Chem. Commun.* **1974**, 615.
- (5) Fujita, E.; Creutz, C.; Sutin, N.; Brunschwig, B. S. *Inorg. Chem.* **1993**, *32*, 2657–2662.
- (6) Hammouche, M.; Lexa, D.; Momenteau, M.; Savéant, J.-M. *J. Am. Chem. Soc.* **1991**, *113*, 8455.

The trichlorostannyl-capped cluster $\text{Ni}_3(\text{dppm})_3(\mu_3\text{-I})(\mu_3\text{-SnCl}_3)$ (**1**) was prepared by the displacement of one capping iodide ligand of $\text{Ni}_3(\text{dppm})_3(\mu_3\text{-I})_2$ ⁷ with SnCl_3^- .⁸ The $^{31}\text{P}\{^1\text{H}\}$ NMR spectrum of **1** shows a singlet at -3.2 ppm that is flanked by satellites due to coupling to the trichlorostannyl group ($J_{\text{P-Sn}} = 93$ Hz). Cluster **1** is the first tin-capped nickel cluster. Puddephatt and co-workers have reported similar trinuclear platinum clusters capped by SnCl_3^- and SnF_3^- ligands.⁹ Cluster **1** is reasonably air-stable as a solid, consistent with a $48e^-$ count.

The corresponding dichlorostannylene cluster $[\text{Ni}_3(\text{dppm})_3(\mu_3\text{-I})(\mu_3\text{-SnCl}_2)](\text{PF}_6)$ (**2**) was prepared by the reaction of **1** with $\text{Ti}(\text{PF}_6)_4$, eq 1.¹⁰ Excess $\text{Ti}(\text{I})$ does not remove a second chloride. The $^{31}\text{P}\{^1\text{H}\}$ NMR spectrum of **2** consists of a singlet at $+1.6$ ppm with satellites arising from P–Sn

- (7) Morgenstern, D. A.; Ferrence, G. M.; Washington, J.; Henderson, J. I.; Rosenhein, L.; Heise, J. D.; Fanwick, P. E.; Kubiak, C. P. *J. Am. Chem. Soc.* **1996**, *118*, 2198–2207.
- (8) $\text{Ni}_3(\text{dppm})_3(\mu_3\text{-I})_2$ (1 g, 0.63 mmol), anhydrous SnCl_2 (0.120 g, 0.63 mmol), and excess NaCl were added to a 250 mL round-bottom flask. THF (100 mL) was then added to the flask. The reaction was allowed to stir for 3 days, during which time a green solid precipitated. The solid was recovered over a medium filter funnel containing a layer of Celite. The solid was then washed with copious amounts of THF and toluene to remove any unreacted $\text{Ni}_3(\text{dppm})_3(\mu_3\text{-I})_2$ or the oxidized form of this complex. The solid was dissolved in a minimal amount of CH_2Cl_2 , and the solution was filtered to remove the remaining NaCl and NaI that were formed in the reaction. The product was then precipitated with 1 equiv of hexanes and collected over a medium filter funnel. Yield: 56%. $^{31}\text{P}\{^1\text{H}\}$ NMR (CD_2Cl_2): -3.2 ppm. PDMS: 1646 [M – Cl⁻]. The purple isomer of **1** results from attempts to reduce the green isomer with Na in THF followed by reoxidation. Crystals of the purple isomer were grown from THF/ether by slow diffusion of ether. $^{31}\text{P}\{^1\text{H}\}$ NMR (THF): -2.1 ppm. PDMS: 1646 [M – Cl⁻].
- (9) Jennings, M. C.; Schoettel, G.; Roy, S.; Puddephatt, R. J. *Organometallics* **1991**, *10*, 580.
- (10) $\text{Ni}_3(\text{dppm})_3(\mu_3\text{-I})(\mu_3\text{-SnCl}_3)$ (0.12 g, .07 mmol) was suspended in $\text{CH}_3\text{-CN}$ (40 mL). $\text{Ti}(\text{PF}_6)_4$ (0.03 g, .09 mmol) was then added to the suspension. After a short period, the solution became homogeneous and orange-brown in color. The solution was filtered through a fine filter funnel to remove the TiI formed in the reaction. The solvent was removed, and the residue was redissolved in THF. The product precipitated upon the addition of an equal volume of hexanes. The solid was collected over a medium filter funnel and washed with excess hexanes. Yield: 100% by NMR. $^{31}\text{P}\{^1\text{H}\}$ NMR (CD_2Cl_2): $+1.6$ ppm. PDMS: 1646.

Table 1. Crystal Data for $[\text{Ni}_3(\mu_3\text{-SnCl}_3)(\mu_3\text{-I})(\text{dppm})_3]\cdot 3\text{THF}$ (**1**) and $w[\text{Ni}_3(\mu_3\text{-SnCl}_2)(\mu_3\text{-I})(\text{dppm})_3][\text{PF}_6]\cdot 3\text{CH}_2\text{Cl}_2$ (**2**)

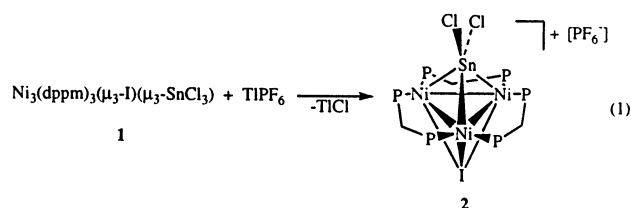
	1	2
formula	$\text{C}_{87}\text{H}_{90}\text{Cl}_3\text{INi}_3\text{O}_3\text{P}_6\text{Sn}$	$\text{C}_{78}\text{H}_{72}\text{Ni}_3\text{SnP}_7\text{ICl}_8\text{F}_6$
fw	1897.61	2045.60
space group	$P\bar{1}$ (No. 2)	$P2_1/n$ (No. 14)
<i>a</i> , Å	14.4869(5)	11.878(4)
<i>b</i> , Å	14.8724(6)	41.277(6)
<i>c</i> , Å	20.4779(9)	17.831(4)
α , deg	69.8506(15)	
β , deg	89.1702(15)	108.06
γ , deg	78.010(3)	
<i>V</i> , Å ³	4043.8(4)	8311(7)
<i>Z</i>	2	4
λ , Å	0.71073	0.71073
ρ_{calcd} , g cm ⁻³	1.558	1.635
<i>R</i> 1 ^a	0.060	0.051
<i>wR</i> 2 ^a	0.140	0.145

^a $R1 = \sum |F_o| - |F_c| / \sum |F_o|$. $wR2 = [\sum w(F_o^2 - F_c^2)^2 / \sum w(F_o^2)^2]^{1/2}$. $w = 1/[^2(F_o^2) + (0.0636P)^2 + 21.9374P]$ where $P = (F_o^2 + 2F_c^2)/3$.

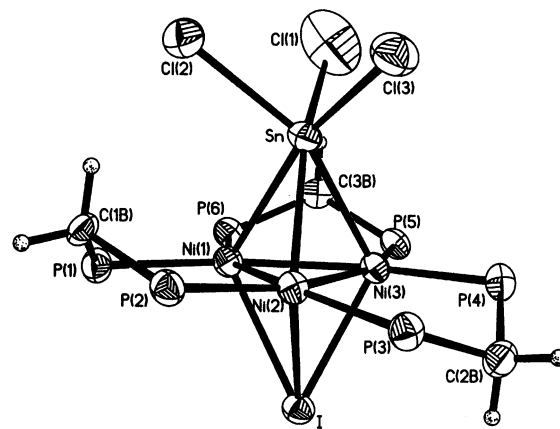
Table 2. Selected Bond Distances (Å)

atom 1	atom 2	distance	atom 1	atom 2	distance
$[\text{Ni}_3(\text{dppm})_3(\mu_3\text{-I})(\mu_3\text{-SnCl}_3)]$ (1)					
I	Ni(3)	2.6549(11)	Sn	Ni(3)	2.6182(12)
I	Ni(2)	2.6613(11)	Sn	Ni(2)	2.6196(12)
I	Ni(1)	2.7173(12)	Sn	Ni(1)	2.6371(11)
Sn	Cl(1)	2.348(4)	Ni(1)	Ni(3)	2.4554(15)
Sn	Cl(3)	2.387(3)	Ni(1)	Ni(2)	2.4599(15)
Sn	Cl(2)	2.497(3)	Ni(2)	Ni(3)	2.4721(14)
$[\text{Ni}_3(\mu_3\text{-SnCl}_2)(\mu_3\text{-I})(\text{dppm})_3][\text{PF}_6]$ (2)					
Ni(1)	Ni(2)	2.4776(19)	Ni(1)	Sn	2.6560(15)
Ni(1)	Ni(3)	2.4849(19)	Ni(2)	Sn	2.4679(15)
Ni(2)	Ni(3)	2.5263(19)	Ni(3)	Sn	2.4809(16)
Ni(1)	I	2.6330(15)	Sn	Cl(1)	2.424(3)
Ni(2)	I	2.6136(15)	Sn	Cl(2)	2.374(3)
Ni(3)	I	2.6047(15)			

coupling ($J_{\text{P-Sn}} = 112$ Hz). Although **2** is a cationic cluster, it too possesses a $48e^-$ configuration because the $:\text{SnCl}_2$ group contributes 1 more electron to the cluster count than the SnCl_3 group of **1**.



Crystals of $[\text{Ni}_3(\text{dppm})_3(\mu_3\text{-I})(\mu_3\text{-SnCl}_3)]$ (**1**) were grown from a 1:1 mixture of CH_2Cl_2 and hexanes. Crystal data are summarized in Table 1. Selected bond distances and angles are compiled in Tables 2 and 3. An ORTEP drawing of **1** is presented in Figure 1. The average Ni–Ni bond length of 2.488(16) Å is within the normal range of Ni–Ni bond distances for nickel clusters of this class.^{7,11,12} The average Ni–I bond length in **1** is 2.656(54) Å, which is also typical of clusters of this class. The three Cl atoms of the $\mu_3\text{-SnCl}_3$ group bear a staggered conformational relationship to the three Ni atoms, resulting in an approximately octahedral

**Figure 1.** ORTEP view of $[\text{Ni}_3(\text{dppm})_3(\mu_3\text{-I})(\mu_3\text{-SnCl}_3)]$ (**1**) showing 50% thermal ellipsoids and atomic labeling. Phenyl rings omitted for clarity.**Table 3.** Selected Bond Angles (deg)

$[\text{Ni}_3(\text{dppm})_3(\mu_3\text{-I})(\mu_3\text{-SnCl}_3)]$ (1)							
Ni(3)	Ni(1)	Ni(2)	60.39(4)	Ni(2)	Ni(3)	Sn	61.87(4)
Ni(1)	Ni(2)	Ni(3)	59.72(4)	Sn	Ni(1)	I	113.37(4)
Ni(1)	Ni(3)	Ni(2)	59.89(4)	Sn	Ni(2)	I	115.85(4)
Ni(2)	Ni(1)	Sn	61.74(4)	Sn	Ni(3)	I	116.12(4)
Ni(3)	Ni(1)	Sn	61.76(4)	Ni(2)	Sn	Ni(1)	55.80(3)
Ni(1)	Ni(2)	Sn	62.46(4)	Ni(3)	Sn	Ni(1)	55.71(3)
Ni(3)	Ni(2)	Sn	61.81(4)	Ni(3)	Sn	Ni(2)	56.33(3)
Ni(1)	Ni(3)	Sn	62.54(4)				
$[\text{Ni}_3(\mu_3\text{-SnCl}_2)(\mu_3\text{-I})(\text{dppm})_3][\text{PF}_6]$ (2)							
Ni(2)	Ni(1)	Ni(3)	61.20(5)	Ni(1)	Ni(3)	Sn	64.67(5)
Ni(1)	Ni(2)	Ni(3)	59.54(5)	Ni(2)	Ni(3)	Sn	59.05(5)
Ni(1)	Ni(3)	Ni(2)	59.26(5)	Ni(3)	Ni(2)	Sn	59.56(5)
Ni(2)	Ni(1)	Sn	57.34(4)	Sn	Ni(1)	I	107.38(5)
Ni(3)	Ni(1)	Sn	57.59(5)	Sn	Ni(2)	I	113.98(6)
Ni(1)	Ni(2)	Sn	64.96(5)	Sn	Ni(3)	I	113.98(5)

coordination at the tin atom. The overall structure of cluster **1** appears qualitatively similar to that of the Pt cluster $\text{Pt}_3(\text{dppm})_3(\mu_3\text{-SnF}_3)_2$, reported by Puddephatt and co-workers.⁹ The ORTEP drawing of **1** (Figure 1) shows that two of the three $\text{Ni}_2(\text{dppm})$ five-membered (Ni–P–CH₂–P–Ni) rings are in envelope conformations with two methylene group “flaps” folded upward toward the capping $\mu_3\text{-SnCl}_3$ group and the third folded down. This same structural motif is observed in Puddephatt’s platinum clusters, as well as in the structure of the stannylene-capped cluster **2**, described in the following paragraph.

Crystals of $[\text{Ni}_3(\text{dppm})_3(\mu_3\text{-I})(\mu_3\text{-SnCl}_2)][\text{PF}_6]$ (**2**) were also grown from a 1:1 mixture of CH_2Cl_2 and hexanes. Crystal data are summarized in Table 2. Selected bond distances and angles are compiled in Tables 2 and 3. An ORTEP drawing of the molecular cation is presented in Figure 2. The average Ni–Ni bond length in **2** is 2.496(26) Å, and the average Ni–I bond length is 2.617(14) Å. The SnCl_2 moiety leans noticeably toward one of the Ni–Ni edges. There is a significant (0.2 Å) difference between one Ni–Sn bond length (Ni(1)–Sn (2.6560(15) Å)) and the other two ((Ni(2)–Sn = 2.4679(15) Å and Ni(3)–Sn = 2.4809(16) Å)). The average of the Ni–Sn bond lengths observed in the trichlorostannyl-capped cluster **1** (2.63(1) Å) is also longer than the average of those in the dichlorostannylene-capped cluster **2** (2.53 Å). The Cl(1)–Sn–Cl(2) angle of **2** (89.65(11)°) is not significantly wider than the average Cl–Sn–Cl angle of **1** (87(4)°). The dichlorostannylene-capped cluster

(11) Ratliff, K. S.; Fanwick, P. E.; Kubiak, C. P. *Polyhedron* **1990**, *9*, 1487–1489.

(12) Ferrence, G. M.; Fanwick, P. E.; Kubiak, C. P. *J. Chem. Soc., Chem. Commun.* **1996**, 1575.

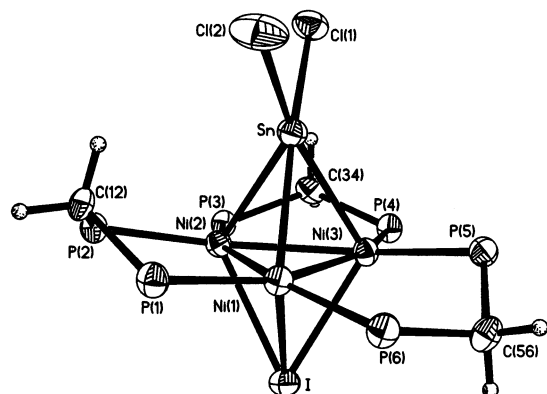


Figure 2. ORTEP drawing of $[\text{Ni}_3(\text{dppm})_3(\mu_3\text{-I})(\mu_3\text{-SnCl}_2)]^+$ (**2**) showing 50% probability ellipsoids. Phenyl rings are omitted for clarity.

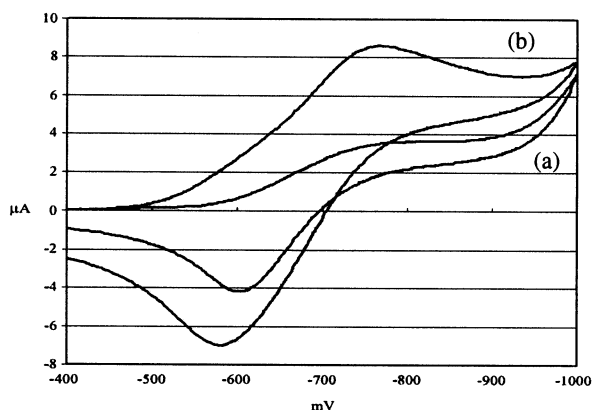
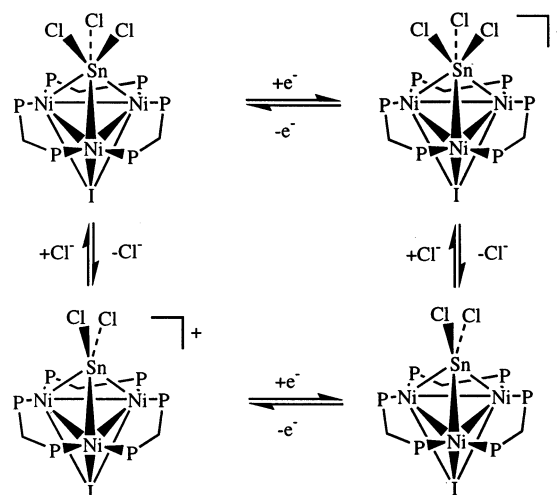


Figure 3. Cyclic voltammogram of $\text{Ni}_3(\text{dppm})_3(\mu_3\text{-I})(\mu_3\text{-SnCl}_3)$ (**1**) in acetonitrile with 0.1 M tetrabutylammonium hexafluorophosphate (TBAH) (a) and with added tetrabutylammonium chloride (b). Potentials referred to SCE.

is the first cluster of this class that is capped by a π -acceptor ligand other than an axially symmetric ligand such as CO or isocyanides.^{7,11} The noted asymmetries in bonding may reflect the fact that the vacant p_z orbital of the stannylene fragment can interact with only one of the two degenerate d π orbitals of the triangular nickel cluster. Cluster **2** appears to present the first example of $\mu_3\text{-SnCl}_2$ coordination, as no related examples for tin have been found in the literature.

The electrochemistry of **1** and **2** is similar to that for the other members of the family of π -acid-capped trimers $[\text{Ni}_3(\text{dppm})_3(\mu_3\text{-I})(\mu_3\text{-X})]^+$ ($X = \text{CO}, \text{CNR}$),⁷ which all display reversible single electron reductions in the vicinity of -1.15 V versus SCE. The electrochemistry of **1** in CH_2Cl_2 is characterized by a single electron reduction near -650 mV versus SCE. In the absence of excess Cl^- , the cyclic voltammetric reduction wave is decidedly irreversible, Figure 3a. Addition of $(n\text{-C}_4\text{H}_9)_4\text{NCl}$ causes the electrochemical

Scheme 1



reduction of **1** to appear chemically reversible. The CV wave becomes nearly symmetrical about -665 mV versus SCE, but the large peak-to-peak separation, $\Delta E_{pp} = 160$ mV, attests to sluggish kinetics for the overall process, Figure 3b. These data suggest that chloride dissociation is occurring from the radical anion $[\text{Ni}_3(\text{dppm})_3(\mu_3\text{-I})(\mu_3\text{-SnCl}_3)]^{\bullet-}$, formed by electrochemical reduction of **1**. Upon prolonged scanning through the CV of **1** in the absence of excess chloride, the irreversible wave near -650 mV gradually evolves into a reversible wave centered at -600 mV. This new wave at -600 mV is identical to that observed in the CV of pure **2**. Thus, **1** and **2** are connected by chloride association/dissociation in both their normal and reduced forms. The chloride dissociation and redox equilibria are summarized in Scheme 1. These studies demonstrate that a site of coordinative unsaturation can be created on a capping ligand of a trinuclear nickel cluster. Our ongoing studies will be devoted to the potential use of an electrophilic tin site and nucleophilic nickel sites in the activation of amphoteric substrates such as CO_2 .

Acknowledgment. We gratefully acknowledge the DOE (Grant DE-FG03-99ER14992) for support and Drs. Eugenio Simon and Peter Gantzel for helpful discussions and presentation of crystallographic results

Supporting Information Available: Tables of crystallographic data collection and refinement parameters, positional and thermal parameters, bond distances and angles for **1** and **2** (CIF). This material is available free of charge via the Internet at <http://pubs.acs.org>.

IC020108A